Changes of the prevailing trade winds over the islands of Hawaii and the North Pacific

Jessica A. Garza,[1] Pao-Shin Chu,[1] Chase W. Norton,[1] and Thomas A. Schroeder[1]

Received 16 September 2011; revised 22 April 2012; accepted 25 April 2012; published 7 June 2012.

[1] Changes in the frequency and intensity of the prevailing northeast and east trade winds from 1973-2009 are analyzed from four land stations in the Hawaiian Islands. A nonparametric robust trend analysis indicates a downward trend in northeast trade wind frequency since 1973. At the Honolulu International Airport, northeast trade wind days usually occurred 291 days per year 37 years ago are observed to occur only 210 days per year in 2009. In contrast, the frequency of the east trade winds has increased over the past 37 years. Comparison of observations from four ocean buoys with land stations for the last 26 years (1984–2009) is presented. The northeast trade frequency is found to decrease for all eight stations while the east trade winds are found to increase in frequency. These results are similar to the longer (1973–2009) data set. Most buoys revealed an increase in trade wind speeds since 1984. The NCEP/NCAR reanalysis II data are used to analyze surface winds and sea level pressure (SLP) over the north Pacific. A northeast to east shifting of winds and an increase in SLP is found to occur from the 1980s to the 2000s epoch. Linear trends in reanalysis II from 1980 to 2009 indicated a strengthening of northeast trade winds over the Hawaiian Islands and in the subtropical eastern North Pacific with an extension of increased northerlies off the California coast. Meanwhile, southeast trades in the eastern North Pacific reduced their strength. Changes in trades in the western Pacific are relatively small.

Citation: Garza, J. A., P.-S. Chu, C. W. Norton, and T. A. Schroeder (2012), Changes of the prevailing trade winds over the islands of Hawaii and the North Pacific, *J. Geophys. Res.*, *117*, D11109, doi:10.1029/2011JD016888.

1. Introduction

[2] The Hawaiian island chain is located approximately between 19° to 22°N and 154° to 160°W. Hawaii is commonly known for its favorable climate and refreshing weather because of its constant warm temperatures, mild humidities, and breezy conditions. The trade wind pattern over the Pacific Ocean is one of the largest and most consistent wind fields in the world [*Wyrtki and Meyers*, 1976]. Present from 85 to 95% of the time in the summer, and from 50% to 80% of the time in the winter [*Sanderson*, 1993], the northeast trades prevail over the islands throughout the year. Persistent northeast trade winds are important to the Hawaiian Islands, because they affect wave height, cloud formation, and precipitation over specific areas of the region. When trades fail to develop the air can become dormant and unpleasant weather can develop, defined by light winds, high humidities and a variation in rainfall distribution [*Schroeder*, 1993].

[3] Using ship based observations and winds stress measurements from 1947 to 1972, *Wyrtki and Meyers* [1976] found a shift in the northeast trade wind direction toward a more zonal orientation between 125°E to 75°W. *Harrison* [1989] analyzed trends from 10 to 30 years of surface winds from several of the central Pacific Islands between 135°E and 125°W. It was shown that between 3°N and 3°S, each island shows decreasing easterlies and increased meridional flow toward the equator, although there is no significant trend in the trades overall. Because there are very few spatial observations of surface conditions in the tropical Pacific, it is difficult to conclude the statistical significance of overall trend patterns in the wind stress fields [*Harrison*, 1989].

[4] In addition to island records, surface winds from individual ship reports were also investigated by *Cardone et al.* [1990] and more recently by *Tokinaga and Xie* [2011]. Multidecadal trends are explained as a result of Beaufort observations versus uncorrected anemometer observations in the data set. This resulted in spurious trends in wind speeds, as suggested by previous research.

[5] *Clarke and Lebedev* [1996] utilized surface atmospheric pressure data as opposed to wind observation data. Because surface pressure data do not depend on varying wind estimation methods and therefore do not suffer from false trends due to incomplete and inhomogeneous wind observations, this data set is preferred. Since zonal pressure difference and zonally averaged equatorial zonal wind stress

[1]Department of Meteorology, School of Ocean and Earth Science and Technology, University of Hawai'i at Mānoa, Honolulu, Hawaii, USA.

Corresponding author: J. A. Garza, Department of Meteorology, School of Ocean and Earth Science and Technology, University of Hawai'i at Mānoa, 2525 Correa Rd., HIG 350, Honolulu, HI 96822, USA. (jagarza11@gmail.com)

0148-0227/12/2011JD016888

(τ_x) are highly correlated; simple surface atmospheric pressure gradients between the eastern and western equatorial Pacific boundaries are effective indicators of τ_x [*Clarke and Lebedev*, 1996]. Based on inferences between zonal pressure differences and τ_x, their results suggested that the equatorial Pacific trades have strengthened in the 1930s, weakened from the late 1930s to late 1950s, strengthened during the 1960s, and have weakened rapidly since the early 1970s. The recent reduction in wind stress has significant implications on oceanic features such as sea level rise and others.

[6] *Vecchi and Soden* [2007] used climate model simulations from the Intergovernmental Panel on Climate Change (IPCC) Assessment Report 4 (AR4) archive to investigate the response of the atmospheric circulation to a warming climate. All models simulated a weakening of the convective overturning of mass in the tropical atmosphere, mainly in the zonally asymmetric component of the flow (i.e., the Walker circulation) as opposed to the zonal-mean component (i.e., the Hadley circulation). The reasons for the strong preference in the Walker circulation are not clear from the analysis. If the Walker circulation becomes weaker as the climate warms, reduction in trade wind strength is expected. Weakening of the trade winds in the Pacific has been documented by observations and general circulation models [*Power and Smith*, 2007; *Collins et al.*, 2010]. Theory and models indicate slowing down of equatorial trade winds leads to weakening of equatorial surface currents, a reduction in Ekman divergence, weakened equatorial Pacific upwelling and a reduced east-west thermocline tilt [*DiNezio et al.*, 2009]. Although these results differ from the positive wind trends suggested by *Cardone et al.* [1990] and *Tokinaga and Xie* [2011], the difference may be due to different sampling periods used in their studies.

[7] Although previous studies such as *Harrison* [1989] and *Tokinaga and Xie* [2011] focused on the change in intensity (magnitude or strength) of trade winds, there are very few works on the change in frequency of occurrence of trade winds in the Pacific Ocean. As a result, a rigorous statistical analysis for detection of trends is employed here. Taken together, this study will investigate changes in both frequency and intensity of the trade winds. The purpose of this study is to use reliable wind observations available over the past 37 years to test whether or not the trade winds over the Hawaiian Islands and surrounding ocean have changed. Time series of the frequency and intensity of the northeast and east trades will be analyzed individually for the given land station locations. Since buoy observations begin in 1984, we will first compare land stations with buoy observations concurrently for the last 26 years. Subsequently we use a longer wind record (since 1973) from land stations to document long-term wind variations. In addition to single-location observational analysis confined to a limited tropical region, surface winds, and sea level pressure from the reanalysis data set and linear trends in surface winds over the North Pacific during the last 30 years are investigated.

2. Data

2.1. Airport Land Stations

[8] Daily wind and sea level pressure (SLP) data from Hawaii airport stations, which can be found on the Web site of the National Oceanic and Atmospheric Administration (NOAA)/National Climatic Data Center (NCDC), are used. Resultant wind speed, resultant wind direction, and SLP are each utilized from the following four airports: Lihue on Kauai Island, Honolulu on Oahu Island, Kahului on Maui Island, and Hilo on the Big Island. Initially, the period of study for the land stations were from 1984 to 2009. Also daily averaged wind speed is used for the land stations for the 26 year period to study the persistence of trade winds. Because the original wind data set is relatively short, an effort was made to extend the 26 year period through a personal contact to NCDC staff meteorologists. Fortunately, digital data were also accessible back to 1973 on a separate file. However, those archive wind data were only available in hourly averaged observations. In order to be consistent with the post 1984 data set, the earlier data had to be converted to resultant wind data by vector calculation. The majority of the stations had nearly 100% of data available with the exception of the Kahului Airport which had 93%.

2.2. Buoy Stations

[9] Hourly wind data from NOAA/National Data Buoy Center (NDBC) ocean buoys, which can be found online, are used. Resultant wind speed and resultant wind direction are obtained for each of the following buoys: Buoy 51001 (B1), Buoy 51002 (B2), Buoy 51003 (B3), and Buoy 51004 (B4). The orientation of the ocean buoys is shown in Figure 1, along with the land stations and the Hawaiian Islands. The longest obtainable period within the buoy data set is from 1984 to 2009, which is consistent with the land stations. In order to have buoy wind data that are comparable to that of the land station daily wind data, the hourly wind buoy data are converted into a daily average for the period of study using resultant vector calculations. The four buoy stations had an average of almost 80% of the data available with B4 the lowest at 76% and B1 the highest at 84%. When analyzing annual buoy trends, no annual value with less than approximately 70% of the data available is used.

2.3. Reanalysis II

[10] Daily SLP, zonal (U) and meridional (V) wind components from NOAA/National Centers for Environmental Predictions (NCEP) /DOE 2 Reanalysis are provided by the NOAA/OAR/ESRL PSD, Boulder, Colorado, USA, from their Web site at http://www.esrl.noaa.gov/psd/. The spatial coverage is on a global T62 Gaussian grid (192 × 94) from 88.542°N–88.542°S, 0°E–358.125°E. Since Reanalysis II data began in 1979, annual wind and SLP data are analyzed from 1980 to 2009 at 10 m and at the surface respectively, for the central and eastern North Pacific from 0°–50°N, 150°E–120°W.

3. Methods

3.1. Definition of Trade Wind

[11] The standard for expressing wind direction in meteorology and most general public weather forecasts is the 8-point compass, which uses the cardinal points of the compass (north, east, south, and west) as well as the ordinal directions (northeast, southeast, southwest, and northwest). In this study, the northeast and east direction intervals of the 8-point compass are considered. A northeast trade wind is defined here as a wind observation between 22.5 and

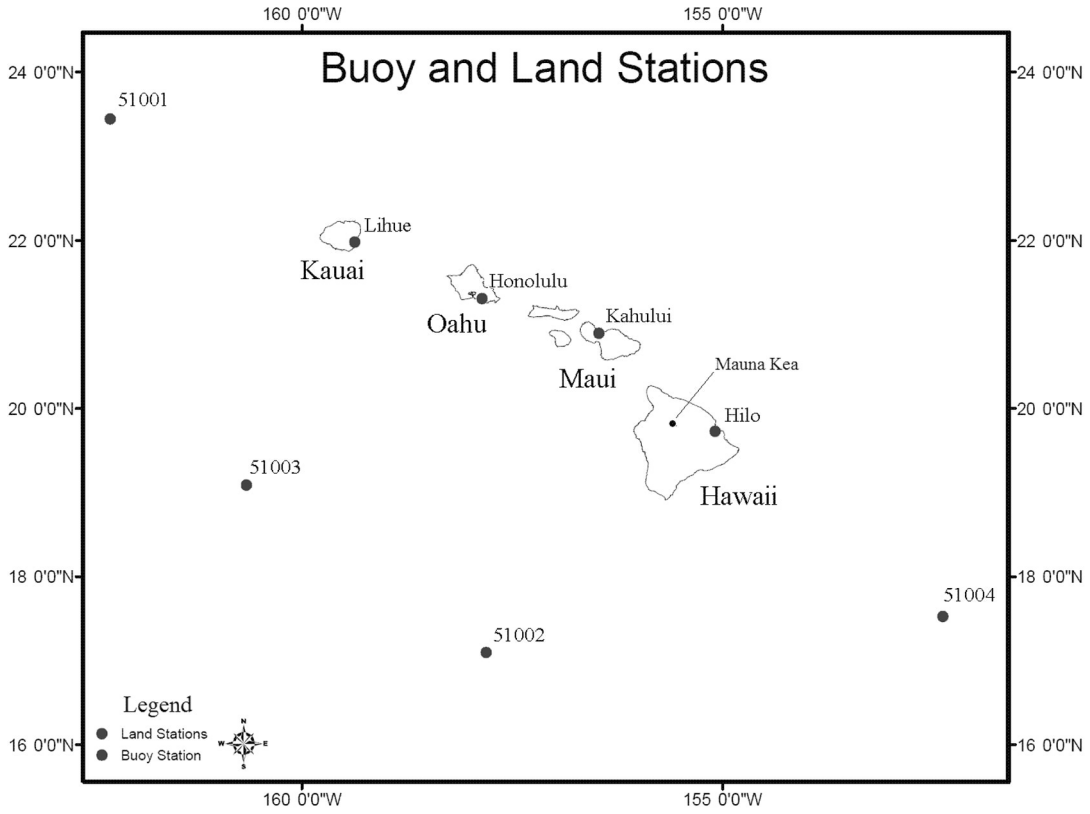

Figure 1. Orientation map of land and buoy stations.

67.5 degrees, while an east trade wind is defined from 67.6 to 112.5 degrees each of which direction encompass a 45 degree angle. In order to analyze trends in northeast and east trade frequency and intensity, an annual trade count and intensity per direction interval is performed for each year.

3.2. Trend Detection Methods and Hypothesis Testing

[12] We will use a nonparametric trend detection method described fully in Appendix A to investigate long-term changes in the frequency and intensity of trade winds at land and buoy stations. These results are summarized in Tables 3, 4, 5, and 6. A simple, parametric regression method is also employed to determine linear trends in trade winds (Figures 4, 5, and 8). Thus, trends are estimated by both parametric and nonparametric methods in this study. A classical nonparametric method called the Wilcoxon-Mann-Whitney test is used to evaluate the SLP difference between two independent samples. This test is described in Appendix B.

3.3. Wind Intensity Corrections

[13] Throughout the course of the last 50 years, there have been various adjustments in anemometer heights at each land station. Table 1 shows the change in anemometer height in meters (m) and the record length for each station. Note that the height change in instrumentation for the Honolulu, Lihue, and Hilo airport are all within 5 m. A +/−5 m displacement typically results in error of less than 5% [*Cardone et al.*, 1990]. However, for a large 12 m modification such as for Kahului airport, a systematic bias in wind speed variations can be expected.

[14] In measured winds, increasing anemometer heights are a major factor in contributing to a spurious upward trend [*Tokinaga and Xie*, 2011]. This same principle applies to decreasing anemometer heights such as the change that took place at Kahului in 1998. Therefore, wind correction calculations are performed for each land station using the wind profile power law equation, so that a true representation of the wind intensity trend can be interpreted accurately. The wind profile power law equation is given by the following:

$$u = u_r \left(\frac{z}{z_r}\right)^p, \tag{1}$$

where u is the estimated new wind speed in meters per second (m s^{-1}) at height z (m), u_r is the known wind speed at reference height z_r, and p = 1/7 (assuming smooth terrain and neutral stability of the atmosphere). The topography

Table 1. Anemometer Height Changes for Each Hawaii Airport Station

Station Name	Dates (Years) of Effectiveness	Height (m)
Lihue Airport	1964–97	6
	Dec 1997–present	10
Honolulu Airport	1962–98	8
	1998–present	10
Kahului Airport	1958–Mar 98	22
	1998–present	10
Hilo Airport	1966–Jan 98	6
	1998–present	10

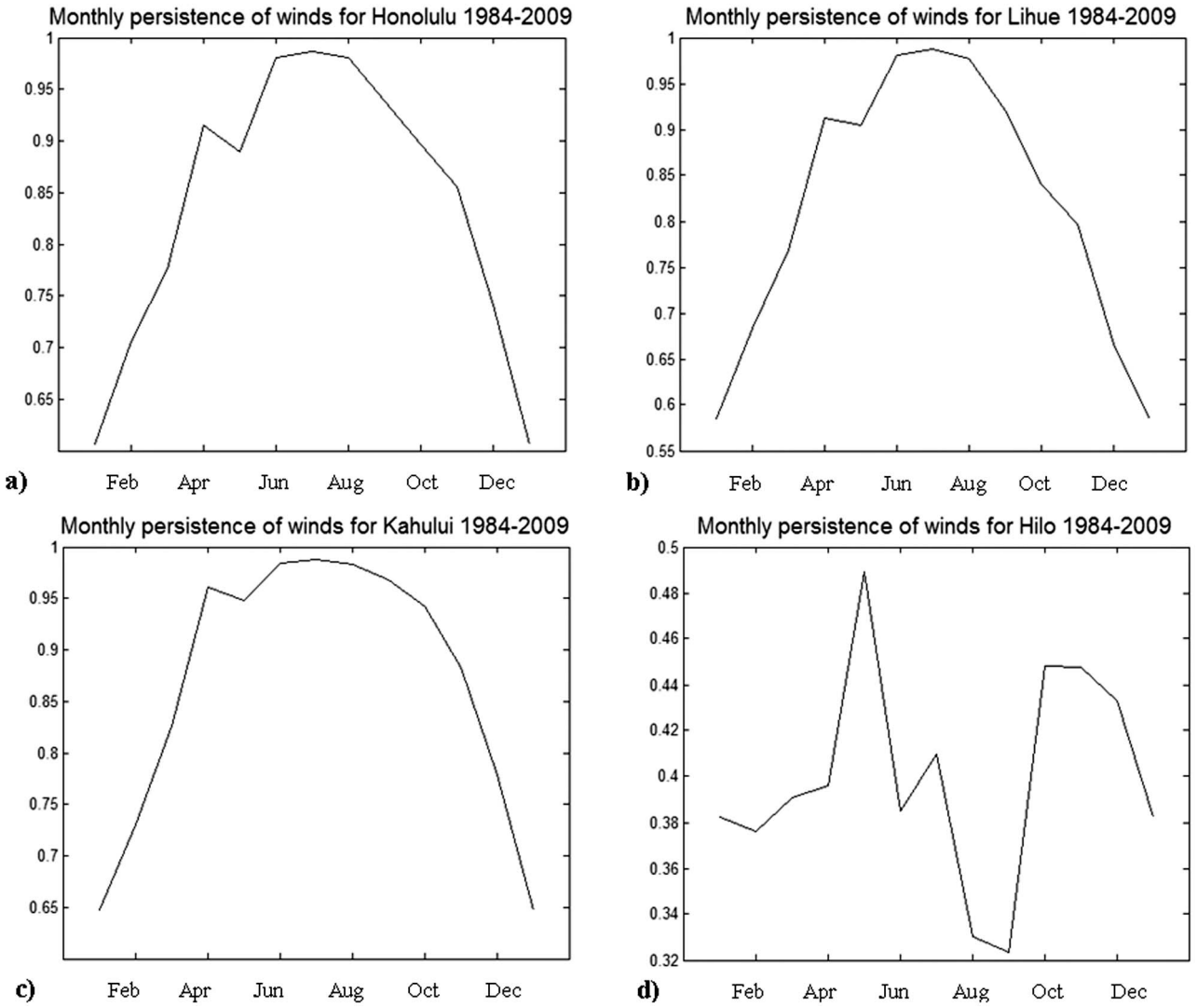

Figure 2. Persistence of winds averaged over 1984–2009 for each month for (a) Honolulu station, (b) Lihue station, (c) Kahului station, and (d) Hilo station. Wind speed (intensity) has been corrected.

surrounding most Automated Surface Observing Systems (ASOS) is normally characterized as aerodynamically very smooth [*Masters et al.*, 2010]. Therefore, when parameters for logarithmic wind profile equations such as zero plane displacement and roughness coefficients are unknown, equation (1) serves as an adequate method for ASOS (i.e., airport) wind corrections. This method for wind speed adjustments at the 10 m anemometer height are carried out for all wind intensity trends, which include the 1973–2009 and the 1984–2009 time periods.

4. Long-Term Climatology of Winds

4.1. Monthly Persistence of Winds

[15] Persistence, also known as constancy or steadiness, is calculated with respect to wind climatology, or the long-term nature of the wind at a particular location. Persistence is defined as the ratio of the wind vector magnitude to the average speed of the wind [e.g., *Glickman*, 2000]. The vector average of a series of wind data describes the resultant wind vector, which incorporates both magnitude and direction. The average speed of the wind, on the other hand, is a scalar quantity, which is simply the average of the magnitude of the individual wind vectors. In using both the magnitude of the resultant wind and the average wind speed, the persistence of wind was corrected for changes in anemometer heights and calculated for each land station for the period of 1984–2009 as shown in Figure 2.

[16] In Figures 2a, 2b, and 2c for Honolulu Airport station (Honolulu), Lihue Airport station (Lihue), Kahului Airport station (Kahului) respectively, notice that the ratio of the resultant vector to the average wind speed is over 60% for the entire 12-months. In the winter months, the ratio stays between 60% and 70%, and then increases to a ratio between 75% and 85% from spring to fall. The most striking feature in these three plots is the extremely high persistence of 90% to almost 100% during the summer months. The strong persistence of winds in the summer months over the general region of Hawaii can be explained by the semi-permanent subtropical high pressure ridge that sits to the northeast of the

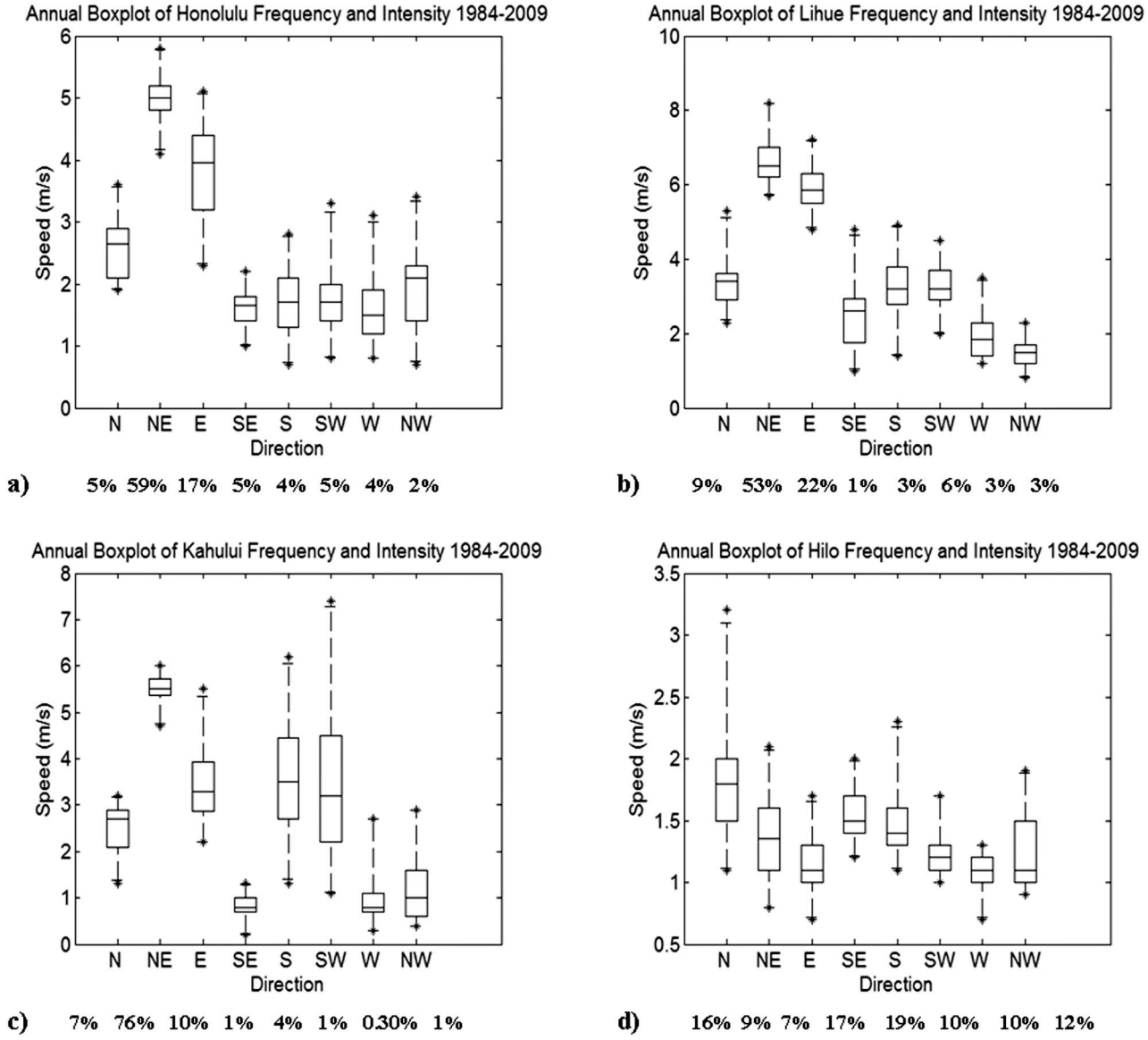

Figure 3. Modified box plots of frequency and intensity for 1984–2009 for: (a) Honolulu, (b) Lihue, (c) Kahului, and (d) Hilo. Wind intensity has been corrected. The maximum and minimum values, the outliers, are indicated by the asterisks on each side of the whiskers. The rectangular box, the Interquartile Range (IQR), bounds the central 50% of the data while the short horizontal line inside the IQR depicts the median of the data set. The wind speeds representing the y-scale vary per station.

island in the summer season, consistently driving northeast trade winds over the island chain. The lower persistence of winds that occurs in the winter months results from the occasional interruption of trade-wind weather caused by various synoptic disturbances, such as the intrusion of upper-level troughs, midlatitude frontal systems, and kona storms [e.g., *Chu et al.*, 1993].

[17] Figure 2d shows tremendous variation in persistence for the Hilo Airport station (Hilo) on the Big Island of Hawaii. Unlike the other three stations which feature overall large ratios (60–90%) and a nearly continuous smooth transition from lower to higher ratios from winter to summer, Hilo depicts generally low ratios (30–50%) and a very inconsistent steadiness of the winds throughout the year. Although Figure 2d is very different from the previous three persistence plots and may look alarming, the results are not very surprising as Hilo is strongly influenced by the katabatic flows from high mountains such as Mauna Kea, which exceeds 4,100 m in elevation. Flow splitting occurs in the Hilo area as the trade winds are forced to move around the island [*Chen and Nash*, 1994] and although large-scale trade winds may play a role, local winds over the Big Island of Hawaii vary considerably from time to time and place to place [*Schroeder*, 1981].

4.2. Frequency of Winds

[18] Figure 3 shows annual modified box plots for Honolulu, Lihue, Kahului, and Hilo for the period of 1984–2009. The eight cardinal directions are plotted on the horizontal x axis against speed in meters per second (m s^{-1})

Table 2. Buoy Station Frequency of Winds for the Period of 1984–2009 for Each Cardinal Direction[a]

	Frequency of Winds			
	B1	B2	B3	B4
N	5%	3%	3%	2%
NE	**24%**	**31%**	**34%**	**39%**
E	**51%**	**61%**	**48%**	**53%**
SE	7%	3%	9%	4%
S	4%	1%	2%	1%
SW	4%	1%	1%	1%
W	3%	0.47%	1%	0.50%
NW	3%	1%	1%	0.38%

[a]NE and E directions are in bold and represent the highest frequencies.

on the *y* axis, while the frequency of each direction interval is labeled below the abscissa. As in *Chu et al.* [1991], 95% of the data lie between the bounded broken lines extending from each side of the box plot.

[19] As shown in Figure 3a, the most common wind at Honolulu is northeasterly, occurring 59% of the time, while the second most common is the east wind direction occurring 17% of the time, out of a total number of (n = 9465) observations. The median wind speed (5 m s^{-1}) and the highest wind speed (5.8 m s^{-1}) are greatest from the northeast. The distribution of the northeast data is fairly symmetric as the extended whiskers and IQR are approximately of equal length. Unlike the northeast and east directions, the other six direction intervals have a very low frequency of occurrence throughout the 26 year period of study.

[20] Lihue, which is shown in Figure 3b, indicates the northeast direction as having the largest frequency of occurrence (53%) out of the total number (n = 9495) of observations. Just like Honolulu, the median wind speed (6.5 m s^{-1}) and the highest wind speed (8.2 m s^{-1}) are also greatest from the northeast for Lihue. The second most frequently occurring wind direction is easterly (22%) which also has a relatively large wind speed compared to the other directions that are characterized by lower wind speeds and frequencies.

[21] For Kahului (Figure 3c) the largest percentage of wind direction is northeasterly (76%), which is the highest among the four stations studied. This is followed by the easterlies (10%) out of a total number (n = 8822) of observations. The northeast data set has wind speeds that range from a minimum of 4.8 m s^{-1} to a maximum of 6.0 m s^{-1}, and a median of 5.5 m s^{-1}. This small range of extremes depicts little variation or high steadiness in wind speed for the prevailing wind direction. The southwest and south winds flows are described not only by large variability but also by very low frequency of occurrence.

[22] Hilo, shown in Figure 3d, does not have a maximum percentage of occurrence representing a dominant wind flow. The northeasterly winds (9%) have a maximum wind speed of 2.1 m s^{-1} and a minimum wind speed of 0.8 m s^{-1} out of a total number (n = 9490) of observations. The east wind interval has even lower maximum and minimum wind speeds as well as a low frequency (7%) of occurrence. Interruptions in trade winds at Hilo due to orographic local effects are shown by the low percentages for each cardinal direction in Figure 2d.

[23] The differences in winds speeds and directions for each station are associated with the station location. For instance, Honolulu is located on the south coast of the island of Oahu (Figure 1). Since the Ko'olau Mountain Range has peaks varying from 500 to 960 m on the island of Oahu and is located below the trade wind inversion which is usually at a height of 2 km [*Cao et al.*, 2007], trade wind flow is directed over the Mountain Range. Although the leeward Honolulu still receives northeast trade winds, the full effect of the northeast trade wind flow is reduced due to the mountain barrier. Meanwhile, since Lihue and Kahului sit on the east-southeast and northern coastline of Kauai and Maui respectively, they experience fresh northeast trade flows without the possible blocking effects of a mountain range, and therefore they encounter larger wind speeds (Figure 3).

[24] In summary, the sum of the northeast and east directions account for 76%, 75%, 86%, and 16% of all wind observations for Honolulu, Lihue, Kahului, and Hilo, respectively as shown in Figure 3. Relative to the other three land stations, Hilo has a very low frequency for the northeast and east directions (16%). Hilo also has the largest variability of frequency percentages for all wind directions, meaning that there is no particular wind compass in which there exists a dominant percentage of a governing wind occurrence for Hilo. Therefore, in the following trend analyses based on the prevailing winds, Hilo will not be used.

[25] As a comparison for wind statistics over the land, Table 2 displays the percentage of wind directions for four ocean buoy stations. The sum of the northeast and east directions account for 75%, 92%, 82%, and 92% of all wind observations for B1, B2, B3, and B4, respectively. Unlike the land stations which have the northeast direction as having the largest frequency of occurrence, the buoy stations show that the east direction is the main wind flow, with the secondary prevailing wind direction being the northeast. Since the Hawaiian Islands are located southwest of the subtropical high pressure ridge axis, the dominant wind flow around the high pressure system is from the northeast, creating favorable environments for northeasterly winds over the islands. Downwind from the islands, over open ocean water, friction is reduced which allows the wind speed to increase. Along with the increase in velocity is an increase in the Coriolis force which causes wind flow to be diverted more to the right in the Northern Hemisphere, allowing for easterly winds observed at the buoy sites. For B1, it is located farther away and downstream from the center of the subtropical high pressure (Figure 1) as such, easterly winds are also dominant.

5. Extended Period of Study: 1973–2009

[26] As explained in section 2, eleven additional years of resultant wind speed and wind direction through instantaneous hourly wind observations were subsequently provided by NCDC. Although the hourly wind observations were available from 1950 for Honolulu, there were a large number of missing years for Lihue prior to 1973. Kahului had hourly wind observations since 1958, but there are a large number of missing years prior to 1973 as well. To be consistent in terms of having the most complete data records, the extended period of study began in 1973. The averaged hourly wind speed and direction were converted into daily resultant wind for 1973–1983 so that the data set may be consistent with the 1984–2009 period. In the Kahului data set there is one missing year in 1997. Figure 4 shows the temporal variations

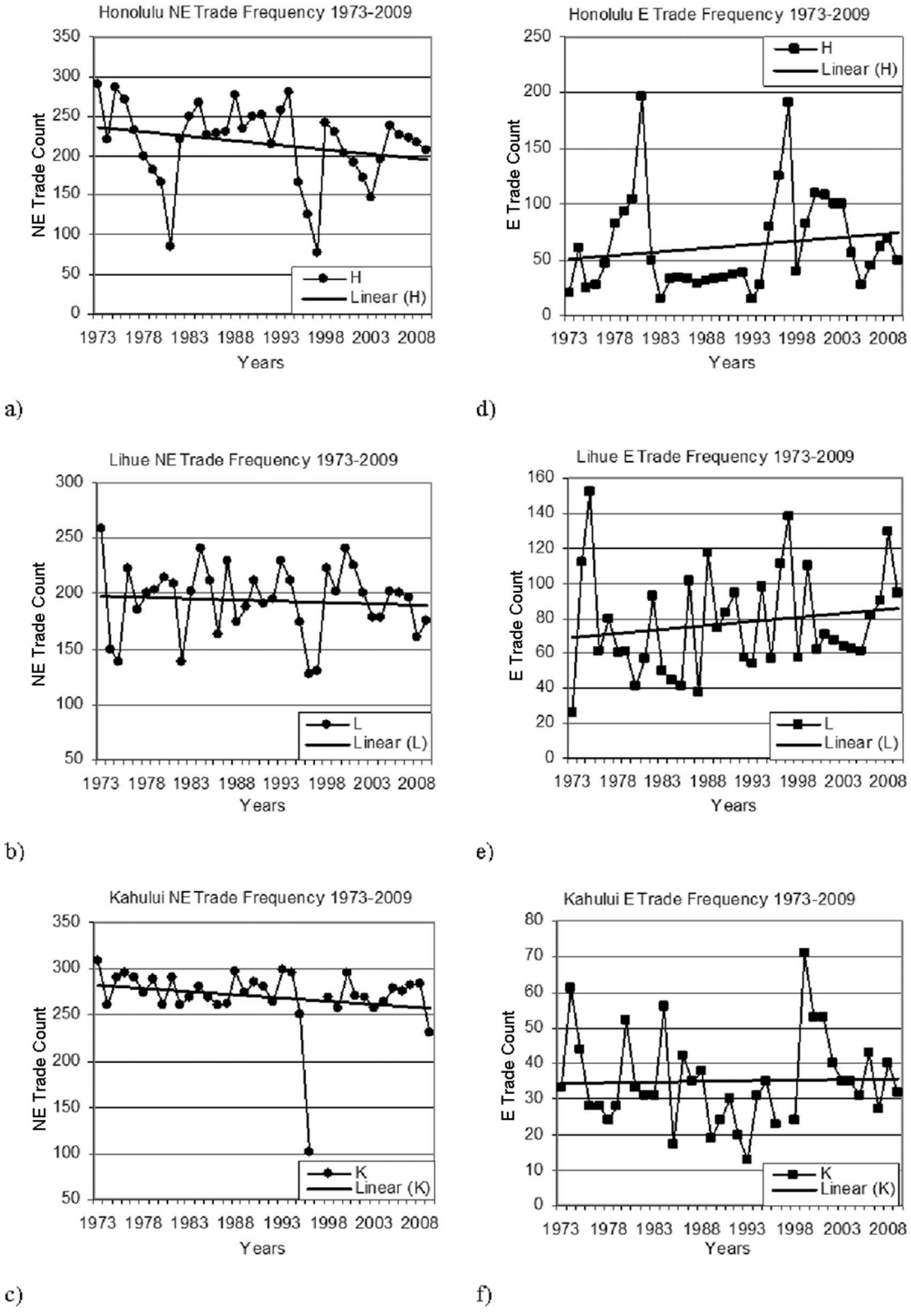

Figure 4. Time series of northeast (NE) and east (E) trade frequency for the period of 1973–2009. Shown are (a) Honolulu NE, (b) Lihue NE, (c) Kahului NE, (d) Honolulu E, (e) Lihue E, and (f) Kahului E. Straight line represents a simple, linear regression line fitted to the record. The northeast trade wind counts in days as shown on the y-scale vary per station.

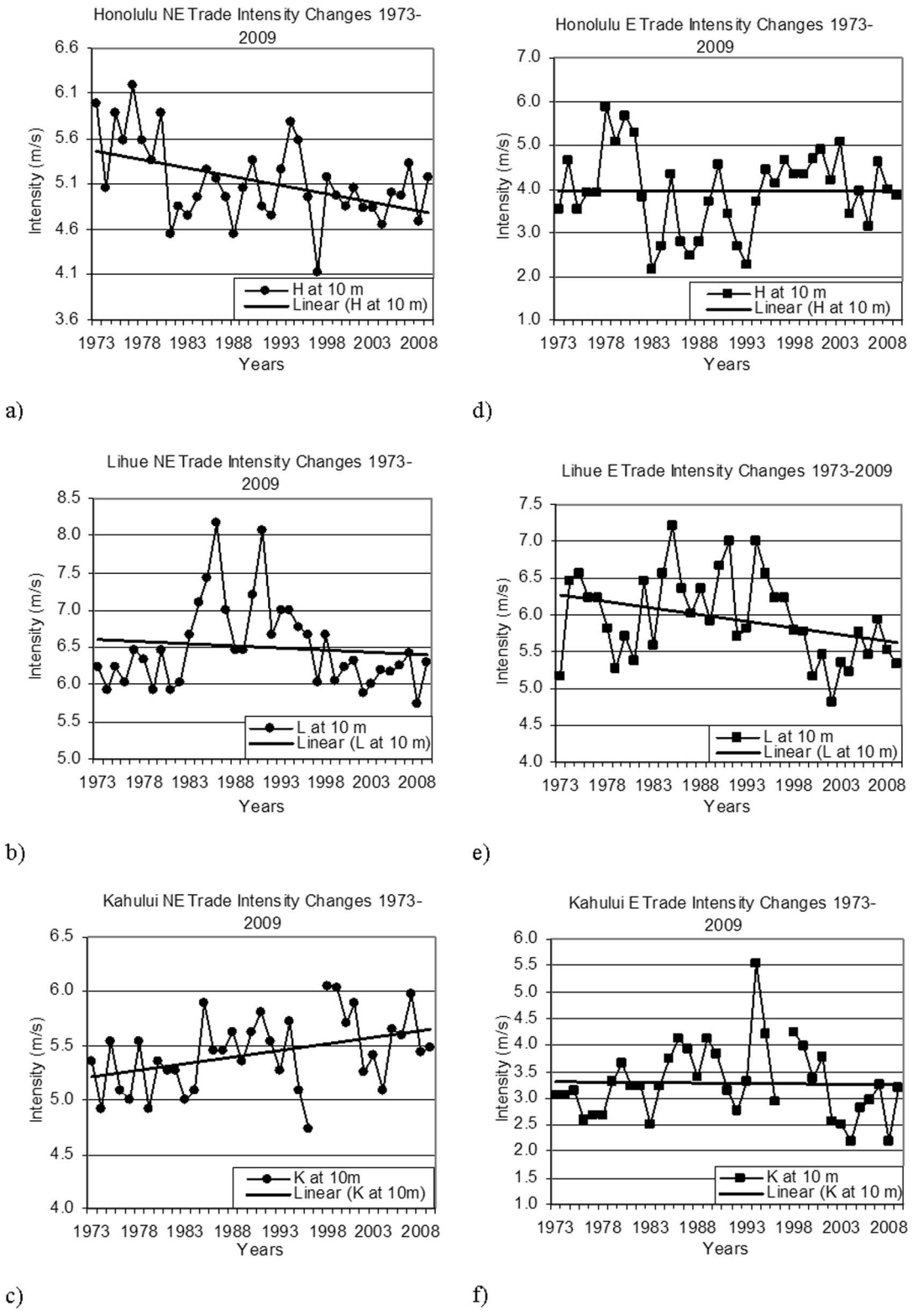

Figure 5. Time series of northeast (NE) and east (E) trade intensity changes for the period of 1973–2009. Shown are wind corrected wind speeds (m s^{-1}) for (a) Honolulu NE, (b) Lihue NE, (c) Kahului NE, (d) Honolulu E, (e) Lihue E, and (f) Kahului E. Straight line represents a simple, linear regression line fitted to the record. The northeast trade wind speeds as shown on the y-scale vary per station.

Table 3. Trend Statistics for NE and E Trade Frequency for the Period of 1973–2009[a]

Time Series	Q
Honolulu NE	**−1.296+**
Lihue NE	**−0.372**
Kahului NE	**−0.279**
Honolulu E	0.735+
Lihue E	0.696
Kahului E	0.091

[a]Q represents the slope of the trend and the plus sign denotes significance at the 10% level. Boldface denotes northeast trades.

of northeast (left panel) and east (right panel) trade frequency from the period of 1973–2009, while Figure 5 shows the northeast and east wind intensity changes with anemometer height corrections.

5.1. Northeast and East Trade Wind Frequency Changes

[27] As shown in Table 3 and Figures 4a, 4b, and 4c, all three land stations exhibit a decreasing trend in northeasterly trade wind frequency. Kahului generally has a large number of northeast trade wind counts with an annual average of 270 trade-wind days for the 37 year period, while the other two land stations have a lower number of counts (annual average of 216 and 194 for Honolulu and Lihue, respectively). Interestingly, all three stations appear to have a drop in counts over the last 37 years. Honolulu, for example, has a decreasing trend and the largest magnitude (−1.3 northeast trade days per year) at the 10% level of significance as shown in Table 3. For Honolulu, the two largest decreases occur in 1981 and 1997 (Figure 4a). 1981 is known as the dry year in Hawaii, which is characterized by an anomalous anticyclonic circulation at the surface as well as an extended eastward 200 hPa jet core, which created subsidence and prohibited trade flows and trade-wind rainfall [*Chu et al.*, 1993]. Without trade-wind induced rainfall, there was a severe drought in 1981. The second major drop in northeast trade days occurs in 1997, during the strongest El Niño event recorded. During El Niño years, strong surface westerly anomalies prevail over Hawaii, which weaken the climatological northeasterly trade winds over the subtropical North Pacific [*Chu and Chen*, 2005]. As a result, trade-wind days become less frequent and there is a substantial reduction in trade-wind rainfall.

[28] A correlation analysis between the Honolulu northeast trade days and the El Niño 3.4 Index for the period of 1973–2009 was conducted based on the annual records. A Pearson correlation of −0.24 was noted, suggesting a weak negative relationship between the two variables tested. That is, when the El Niño index is large and positive, or an El Niño condition, northeast trade-wind days are generally reduced. However, this negative correlation is not significant at the 5% level. This weak correlation is supported by the other large El Niño event such as 1982/83, during which northeast trade-wind days do not decrease sharply, as they do in 1997 (Figure 4a). Detailed diagnostic studies are necessary for understanding causes of changes in trade-wind frequency between these two strong El Niño events. In order to determine whether or not these frequency trends still exits during the months in which the trade winds are most persistent, an analysis of the summer months of June, July, and August has been performed. The trend statistics for *northeast* trade wind frequency (not shown) indicates that the Honolulu and Lihue stations both show decreasing trends consistent with previous results based on the annual records (Table 3).

Table 4. Trend Statistics for Northeast and East Trade Intensity Changes for the Period of 1973–2009 After Wind Corrections[a]

Time Series	Q
Honolulu NE	**−0.018***
Lihue NE	**−0.002**
Kahului NE	**0.013***
Honolulu E	0.005
Lihue E	−0.021*
Kahului E	0.000

[a]Q represents the slope of the trend. Boldface denotes northeast trades. An asterisk denotes significance at the 5% level.

Table 5. Trend Statistics for Northeast and East Trade Frequency for the Period of 1984–2009[a]

Time Series	Northeast Q	East Q
Honolulu	−2.00*	1.417*
Lihue	−0.833	1.00
Kahului	−0.172	0.333
Buoy 51001	−0.162	2.00+
Buoy 51002	−3.125	3.50+
Buoy 51003	−3.087	6.07**
Buoy 51004	−3.36*	4.89**

[a]Q represents the slope of the trend, and a plus sign, a single asterisk, and a double asterisk denote significance at the 10%, 5% and 1% level, respectively.

[29] Unlike the northeast trade-wind frequency, the east trade-wind frequency for 1973–2009 all reveal increasing trends as shown in Table 3 and Figures 4d, 4e, and f. Kahului generally has a low number of east trade wind counts (an average of 35 east trade days per year), while Honolulu and Lihue have a large number of east trade wind days (average of 63 and 77 for Honolulu and Lihue respectively). Interestingly, the two largest peaks in east trade counts occur for Honolulu in 1981 and 1997 (Figure 4d), which seem to make up the deficiency of northeast trade wind days for those two particular years (Figure 4a). Overall, for the extended period of study the northeast trade frequency shows decreasing trends, while the east trade days are shown to be increasing with time.

5.2. Northeast and East Trade Wind Intensity Changes With Wind Corrections

[30] Figures 5a–5c show the time series for the northeast trade intensity changes with wind corrections and the right

Table 6. Trend Statistics for Northeast and East Trade Intensity Changes for the Period of 1984–2009 After Wind Corrections[a]

Time Series	Northeast Q	East Q
Honolulu	−0.007	0.047*
Lihue	−0.054***	−0.054***
Kahului	0	−0.052*
Buoy 51001	0.034+	0.038**
Buoy 51002	−0.010	0.035*
Buoy 51003	0.015	0.024
Buoy 51004	0.030+	0.052

[a]Q represents the slope of the trend, and a plus sign, a single asterisk, a double asterisk, and a triple asterisk denote significance at the 10%, 5%, 1%, and 0.1% level, respectively.

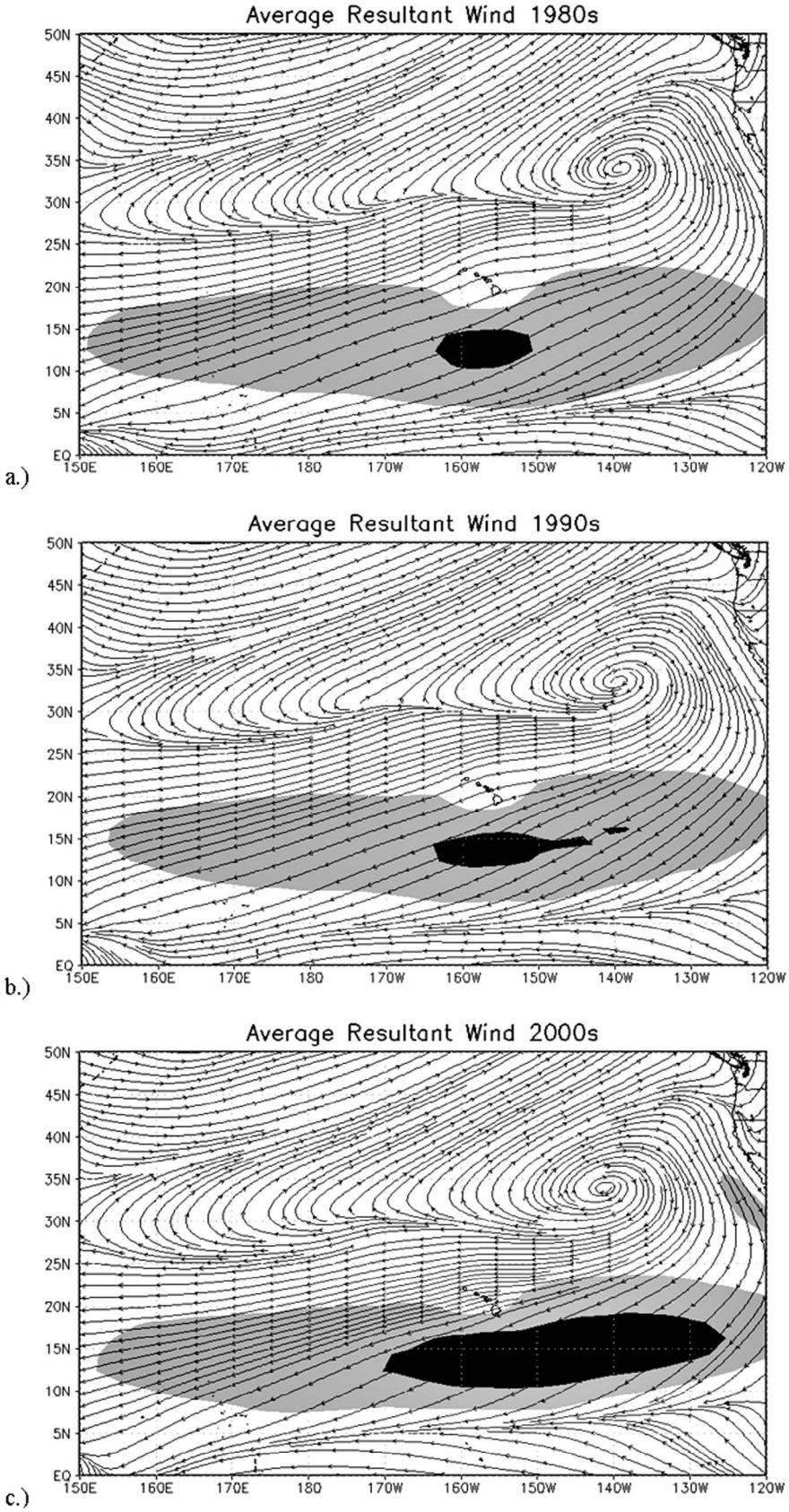

Figure 6. Annual averaged 10 m resultant wind and magnitude for the central/north Pacific for the period of (a) 1980–1989 (1980s), (b) 1990–1999 (1990s), and (c) 2000–2009 (2000s). Grey (black) regions represent wind speeds of 7–8 m s^{-1} (greater than 8 m s^{-1}).

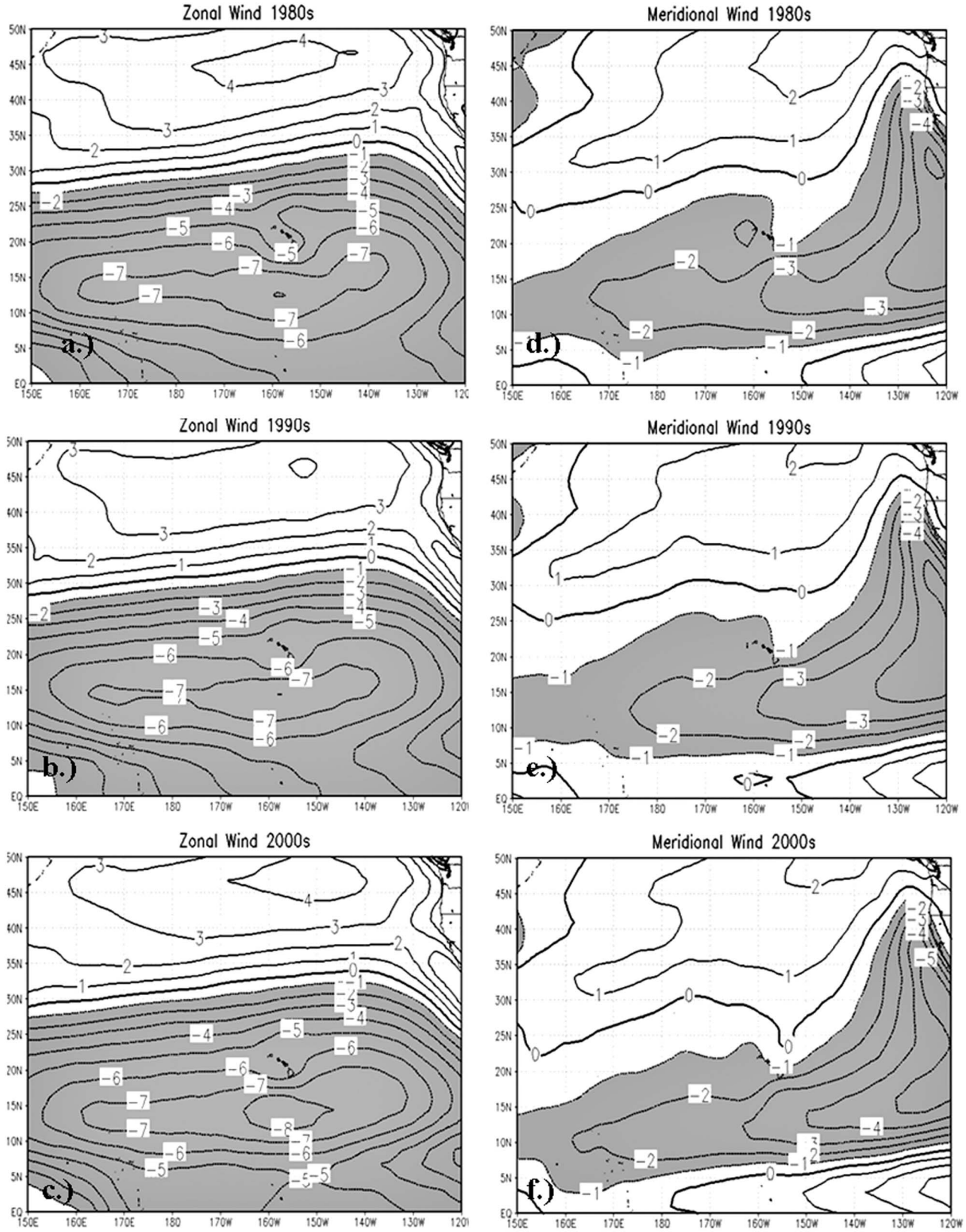

Figure 7. Zonal wind for: (a) 1980s epoch, (b) 1990s epoch and (c) 2000s epoch. Meridional wind for: (d) 1980s epoch, (e) 1990s epoch and (f) 2000s epoch. Grey (white) regions represent negative (positive) component wind values (m s^{-1}).

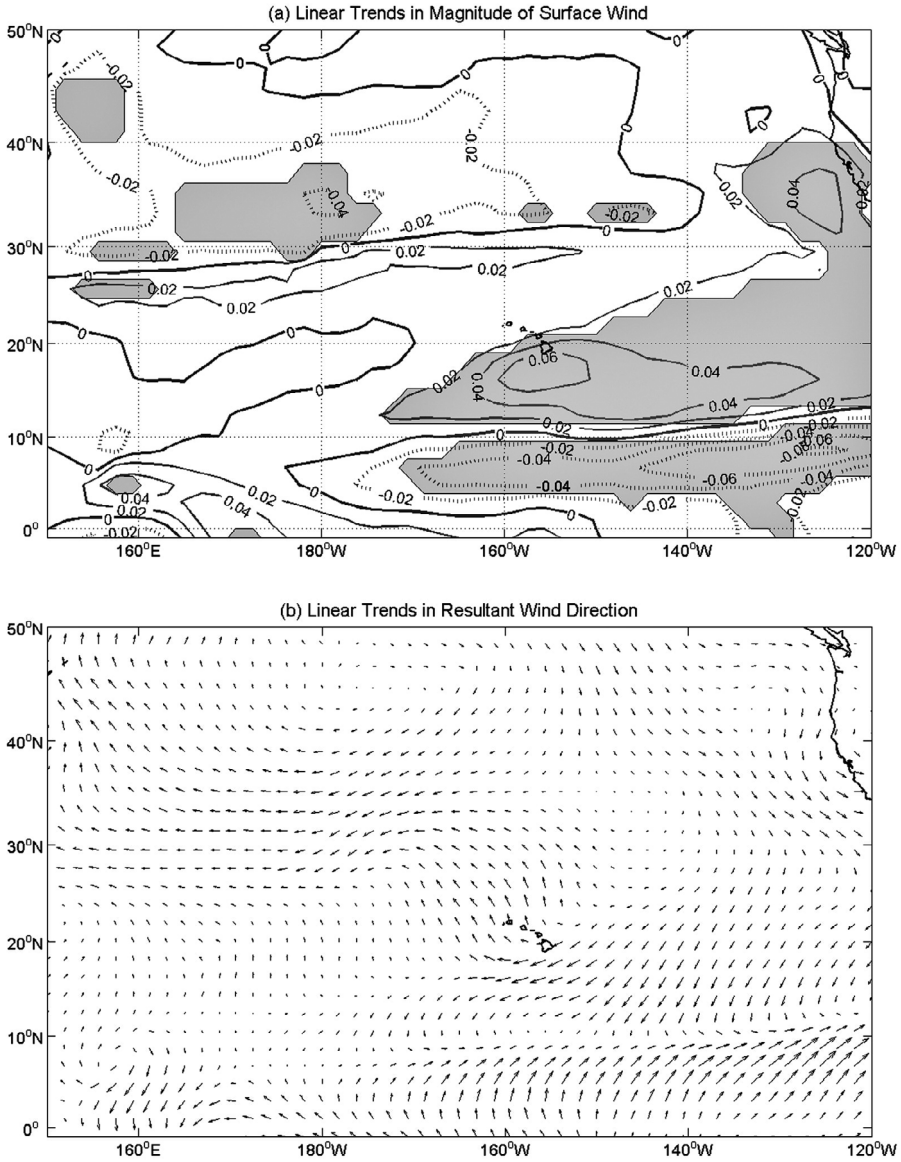

Figure 8. Linear trends of surface wind (m s^{-1}) from 1980 to 2009. (a) Linear trends in magnitude of wind. Solid (dashed) contours represent increases (decreases) in wind speed. Areas of gray represent statistical significance at the 5% level. Unit of trend is m s^{-1} yr^{-1}. (b) Linear trends in vector winds.

column shows the time series for the east trade intensity changes along with wind corrections for the period of 1973–2009 for all land stations. All plots show the calculated wind speeds at the 10 m anemometer height for the northeast and east intervals.

[31] Table 4 lists the trend for the northeast/east intensity changes with wind corrections over the last 37 years. The northeast trade wind intensity has decreased for Honolulu (statistically significant at the 5% level) and Lihue. Opposite to the two other land stations, Kahului is shown to have an increase of 0.013 m s^{-1} per year and is statistically significant at the 5% level also. These changes are also seen in Figure 5c. In Table 4, the east trade wind intensity, which also has mixed signals, shows an increasing trend for Honolulu, a decreasing and statistically significant trend at the 5% level for Lihue, and no change for Kahului.

[32] Since buoy data began in 1984, we used land stations from 1984 to 2009 to make a direct comparison with buoy observations. For these shorter records (Table 5), changes in northeast and east trade wind frequency at land stations are consistent in sign to those of the buoy stations. That is, they all show a decreasing trend in northeast trade frequency and an increasing trend in east trade frequency, regardless of the land or buoy stations. For the northeast wind intensity (Table 6), both Lihue and Honolulu show a decrease while Kahului has a zero trend. Buoy stations experience an increase in northeast wind intensity, with the exception of B2. For changes in east wind intensity, Lihue and Kahului

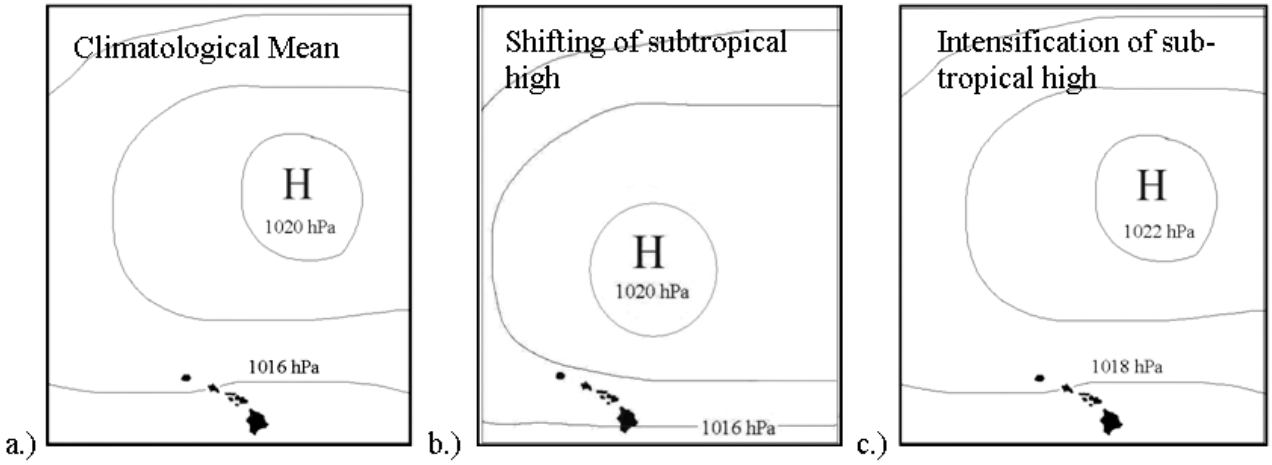

Figure 9. Schematics showing (a) climatological location of subtropical high pressure to the northeast of islands, (b) possible shifting of ridge axis, and (c) possible intensification of ridge axis.

exhibit a decrease, while Honolulu now shows an increase. Changes in east trade intensity for buoys are found to increase uniformly since 1984.

6. Large-Scale Circulation Features Associated With Changes in Trade-Wind Frequency

[33] As depicted in Figure 4 and Table 3, the frequency of northeast trade winds observed at land stations has been declining noticeably since 1973. In this section, we analyzed large-scale sea level pressure and surface wind for each decade to provide understanding of the long-term change in trade-wind frequency. To determine changes in decadal circulation fields in the North Pacific, the resultant wind and SLP data from reanalysis II were divided into three epochs as follows: 1980–1989 (1980s), 1990–1999 (1990s), and 2000–2009 (2000s). Each epoch was plotted over a large-scale domain from 150°E to 120°W and from the equator to 50°N. Changes in wind direction, magnitude (m s^{-1}), and SLP over each epoch are represented by the streamlines and isobars respectively.

6.1. Winds

[34] In the 1980s plot, the anticyclonic flow of the surface wind can be seen around the subtropical high pressure ridge axis to the northeast of the Hawaiian Islands (Figure 6a). The magnitude of the wind is between 5 and 6 m s^{-1} over the islands and the flow is from the northeast. In the 1990s plot, there is no dramatic indication of a shift in wind flow over the islands (Figure 6b). In the 2000s plot the direction of the wind flow shifts to a more east-northeast orientation while the magnitude of the winds (5–6 m s^{-1}) appears to remain unchanged over the majority of the islands (Figure 6c). Just south of the Island of Hawaii there is an increase in wind speeds attaining 7–8 m s^{-1}. A more pronounced increase in wind speeds greater than 8 m s^{-1} occurs south of the island chain between 170°W and 130°W and 12°N and 17°N.

[35] To better examine changes in wind flow over the region, zonal and meridional wind components for each decade are plotted in Figure 7. Viewing both wind components from 25°N and poleward, there are no major changes from the 1980s to the 2000s. The noticeable alterations in zonal and meridional wind components occur around and below the Hawaiian Islands. The region between 15°N−10°N over all three epochs shows increases in the easterly wind component from −6 to −7 m s^{-1} in the 1980s to −8 m s^{-1} in the 2000s (Figures 7a and 7c). When examining changes in the meridional component over the Hawaiian Islands from 15°N–25°N, the zero line dips southward, indicative of a weakening of the northerly component from the 1980s to 2000s (Figures 7d–7f).

[36] A linear trend analysis of surface winds was conducted in order to determine if surface wind speeds over the North Pacific have changed over the past thirty years. In Figure 8a, shaded areas represent linear trends which are statistically significant at the 5% level. The greatest changes in wind speed near the Hawaiian Islands are given by an increased magnitude of 0.06 m s^{-1}. Also note the large increase in northeast trades over the subtropical eastern North Pacific with an extension of increased northerlies off the California coast. Decreases in southeast trade wind speed are found equatorward of 10°N between 120°W and 170°W. Note that the increases in the magnitude of the northeast trade winds are consistent with the intensity changes from the buoy stations which are found to increase (with the exception of B2) over the same period (Table 6). Changes in trade wind strength in the western Pacific are relatively small. Figure 8b describes the linear trends in vector winds which correspond well to the changes in the mean meridional and zonal wind components for each epoch (Figure 7). The group of northeast wind vectors below and to the southeast of the Hawaiian Island chain can be described by the increased zonal flow from the 1980s epoch to the 2000s epoch shown in Figures 7a–7c. In Figure 8b, the area of southeast wind vectors found to the northwest of Hawaii is explained by the weakening of the northerly component previously illustrated in Figures 7d–7f.

[37] Since we know the large-scale surface wind patterns of the tropical North Pacific have changed over the past three decades, and since surface wind flows are governed by pressure gradients, we can hypothesize two possible scenarios in SLP modifications associated with changes in wind

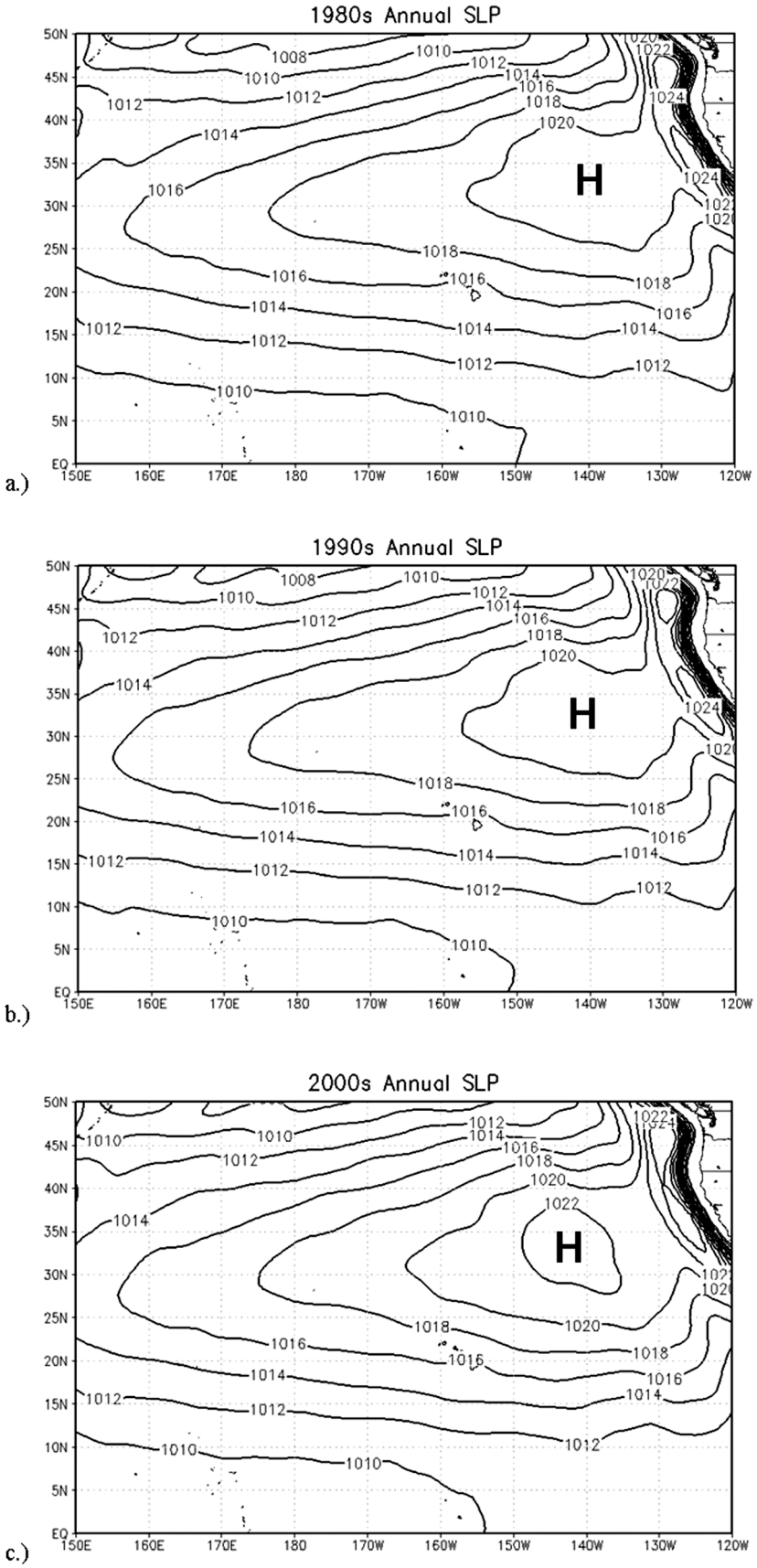

Figure 10. Annual averaged SLP (hPa) for the central/north Pacific for the period of (a) 1980–1989 (1980s), (b) 1990–1999 (1990s), and (c) 2000–2009 (2000s).

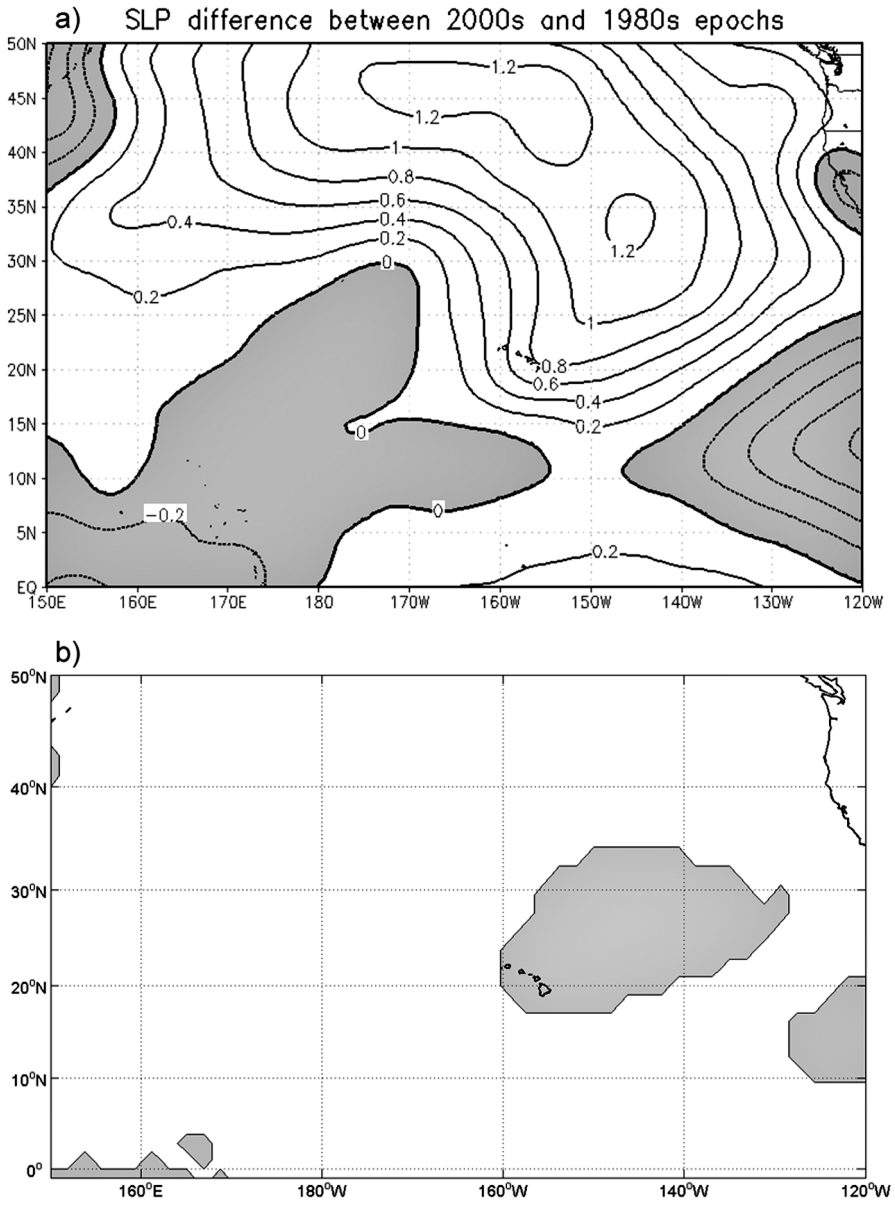

Figure 11. (a) Difference in SLP between the 2000 and 1980 epochs (2000s–1980s). Grey (white) regions indicate negative (positive) values. (b) The non-parametric Wilcoxon-Mann-Whitney test for the difference in SLP between the 2000 and 1980 epochs (2000s–1980s). The gray regions denote areas that are significant at the 5% level.

direction as shown in Figure 9. A climatological mean SLP pattern is depicted in Figure 9a, while Figure 9b denotes a westward shift in the subtropical high pressure, and Figure 9c represents intensification of the subtropical high pressure system. Both changes in the high pressure system location and intensity have implications on wind direction and wind speed over Hawaii. It will now be of interest to investigate which scenario associated with large scale SLP changes is more likely.

6.2. SLP

[38] The subtropical high pressure ridge, shown in Figure 10a, is plotted for the 1980s and is centered about 140°W and 33°N, with the largest isobar reading at 1020 hPa. The perturbed 1016 hPa isobar sits across the island chain over Oahu. Meanwhile the 1990s plot shows a small westward extent of the high pressure system (Figure 10b). The most noticeable changes are seen in the 2000s plot which shows intensification of the high pressure center from 1020 hPa in the 1980s and 1990s, to 1022 hPa in the 2000s (Figure 10c). The center of the subtropical high is close to 142°W and 33°N in Figure 10c. An obvious shifting of the subtropical ridge is not indicated in the plots, although westward movement of the 1020 hPa isobar from the 1980s to the 2000s is noticeable. The intensification of the ridge is seen over the island chain as the 1017 hPa isobar (not

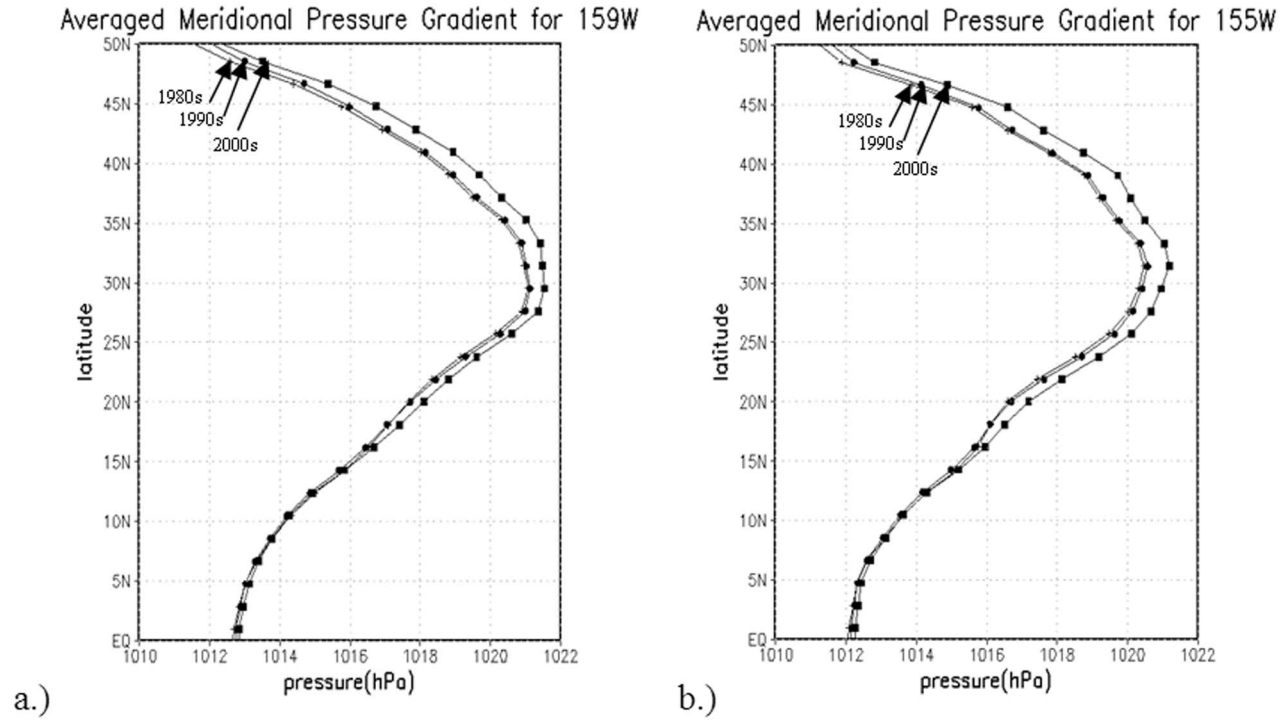

Figure 12. (a) Meridional profiles of SLP gradient for 159°W. (b) Same as in Figure 12a but for 155°W. Cross, circle, and square lines indicate the 1980s, 1990s, and 2000s epochs respectively.

shown) now sits over Kauai and the original 1016 hPa contour that was once located across Oahu is now pushed further southward just to the north of the island of Hawaii (Figures 10a and 10c). This is indicative of stronger surface atmospheric pressure for Hawaii along with a possible shifting of winds due to the more zonal orientation of the 1016 hPa isobar as shown from Figures 10a–10c.

[39] To see a clear visual picture on how much the SLP has intensified from one epoch to another, Figure 11a shows the differences in pressure between the 2000s and 1980s epochs. Positive anomalies are found between 20°N–50°N with increases in SLP ranging from 0.2 to 1.2 hPa in the recent epoch. The greatest increase in SLP (1.2 hPa) is shown over the central location of the subtropical ridge between 30°N–45°N and 140°W–170°W. Over the Hawaiian Islands, the increase in SLP from the 1980s to the 2000s epochs is shown to be 0.6–0.8 hPa. The corresponding nonparametric Wilcoxon-Mann-Whitney test shown in Figure 11b provides indication that the difference in the SLP from the 1980s to the 2000s is statistically significant at the 5% level. Latitudinal profiles (Figures 12a and 12b) of these increases were calculated for longitudes 159°W and 155°W and show noticeable increases in SLP that take place between 20°N–50°N in the 2000s epoch.

7. Conclusions

[40] Trade winds around the Hawaiian Islands are persistent, with higher steadiness in summer rather than winter. The prevailing wind over the Hawaiian Islands is the northeast trade wind (between 22.5°–67.5°) averaging around 63% for Honolulu, Lihue, and Kahului. Due to orographic effects, Hilo does not reveal large frequencies of northeast winds or constancy of winds from a specific direction. In contrast to the land stations, the buoys exhibit the east trade wind (between 67.6°–112.5°) as the prevailing wind averaging about 53% for all four buoy stations. Although the North Pacific trade wind is one of the most consistent wind fields on the globe, interannual variation in wind speed and direction occurs due to synoptic disturbances and climatic events, such as El Niño and La Niña.

[41] Changes in the northeast and east frequency for all land stations display the same signals for the 1973–2009 period, with a decrease (increase) in northeast (east) frequency. For example, northeast trade wind days which occurred 291 days per year 37 years ago at the Honolulu International Airport, now only occur 210 days per year. The drop in the annual northeast trade-wind frequency is also observed at Lihue and Kahului Airports since 1973, although the decrease is not as large as that for Honolulu. Intensity changes for this extended period are inconsistent in signal. The northeast intensity decreased at Honolulu and Lihue, while it increased at Kahului. For the east wind, its intensity decreased at Lihue, while a slight increase occurred at Honolulu. Kahului indicates no change in easterly wind intensity over this time period.

[42] For the 1984–2009 period, when both land and buoy observations were available, the trade frequency from the northeast direction is again found to decrease, while the trade frequency from the east direction is found to increase. This result is similar to what was found in the longer records (1973–2009). For buoy stations for the period of 1984–2009, trade frequency from the northeast direction is found to decrease ubiquitously while the trade frequency from the east direction is found to increase. In addition, northeast and east intensity changes from buoy stations are found to increase, with the exception of B2.

[43] The northeast and east frequency time series suggests a shifting of winds over the Hawaiian Islands. If less northeasterly winds are being observed while more easterly winds are occurring, this indicates shifting of the large-scale pressure and wind patterns. This leads to thoughts as to what may be causing changes in wind flow and pressure. Since Hawaii's prevailing trade winds are governed by the subtropical ridge located to the northeast of the islands, it is beneficial to examine any identifiable shifts in the location of the large-scale circulation over the central/eastern Pacific. Reanalysis II data showed very faint alterations in wind and SLP from the 1980s epoch to the 1990s epoch. Changes in surface wind strength over the last 30 years are given by linear trend analysis which shows increases in northeast trades over the island chain and in the subtropical eastern North Pacific. In contrast, southeast trades in the eastern North Pacific reduced their strength over the last 30 years. Changes in surface wind in the western North Pacific are relatively small. Intensification of the subtropical ridge located to the northeast of the Hawaiian Islands is described by the increase in SLP (1.2 hPa) between 30°N–45°N and 140°W–170°W. Over the islands, the increase in SLP from the 1980s to 2000s epochs is shown to be between 0.6 and 0.8 hPa. Although this difference in SLP seems to be small, it is considerable when viewed in the context of multiyear means between two decades.

8. Discussion

[44] Although the detection of changes in trade-wind intensity for the land stations is most challenging, this study captures the large-scale pattern of intensity changes over the past 30 years. Since wind speeds over the Hawaiian Islands are more variable than wind direction (perhaps due to local wind effects influenced by terrain and diurnal variations of the wind), it is possible that intensity trends are sensitive to small changes in wind speed. More specifically, land station data originate from airport surface observations systems which allow the local exposure of the airport runways to influence wind intensities more so than wind direction over a diurnal period due to daytime heating and nighttime radiational cooling. In addition, mesoscale effects including orographic features of the Hawaiian Islands such as the West Maui Volcano are also significant in producing a variation of wind directions due to the diurnal cycle of the anabatic and katabatic wind.

[45] Because of these local orographic factors, it is beneficial to compare airport station observation results to that of reanalysis II data. The way in which the data are compared differs from the procedure used with the land station data. Airport station observations were transformed into annual northeast and east wind data sets, whereas the reanalysis II data were plotted as a whole, and differences in wind direction can be seen throughout decadal epochs as opposed to annual changes. Although the methods of data analysis differ, the overall objective was to obtain observable changes over the large-scale domain throughout the last 30 years. In utilizing the reanalysis II data, it is shown that throughout the past three decades, wind speeds have increased south of the Hawaiian Island region. These increases are also found in buoy observations and are similar to those of *Tokinaga and Xie* [2011] who found positive trends in increasing trades for the north Pacific and central tropical Pacific in their WASWind data set from 1987 to 2006. Performing climatological studies in the region of Hawaii are challenging due to many factors such as: the steadiness of the trade winds over the Pacific Ocean, orography and diurnal cycles over the islands, as well as natural variability which include ENSO and the Pacific Decadal Oscillation (PDO). Because reanalysis II supports changes in wind direction and increases in wind speed over the Hawaiian Island region throughout each epoch, similar to that of buoy wind observations and intensity changes over the past 26 years, this study is successful in capturing ubiquitous signals in trade wind frequency and intensity in the tropical islands of Hawaii and the north Pacific through a rigorous trend detection analysis.

Appendix A: A Nonparametric Trend Analysis

[46] Using the nonparametric Mann-Kendall test, the presence of a monotonic increasing or decreasing trend is detected and the significance of the trend is tested. Assume the data values of the time series obey the model,

$$x_i = f(t_i) + \varepsilon_i, \tag{A1}$$

where $f(t)$ is a monotonic increasing or decreasing function of time and the residuals ε_i are assumed to originate from the same distribution with zero mean. The existence of a statistically significant trend is obtained by the Y statistic as follows:

$$Y = \begin{Bmatrix} \dfrac{S-1}{\sqrt{\mathrm{VAR}(S)}} & \text{if} \quad S > 0 \\ 0 & \text{if} \quad S = 0 \\ \dfrac{S+1}{\sqrt{\mathrm{VAR}(S)}} & \text{if} \quad S < 0 \end{Bmatrix}, \tag{A2}$$

[47] If the Y value is positive (negative) this is an indication of an upward (downward) trend. In equation (A2), S is defined by the following:

$$S = \sum_{k=1}^{n-1} \sum_{j=k+1}^{n} \mathrm{sgn}(x_j - x_k), \tag{A3}$$

$$\mathrm{sgn}(x_j - x_k) = \begin{cases} 1 & \text{if} \quad x_j - x_k > 0 \\ 0 & \text{if} \quad x_j - x_k = 0 \\ -1 & \text{if} \quad x_j - x_k < 0 \end{cases}, \tag{A4}$$

where n represents the number of years, x_j and x_k are the annual values in years j and k respectively, and $j > k$. Because the validity of the Y may be reduced if there are several tied groups in a time series, the variance takes into account the number of ties that may be present and is computed based on the following:

$$VAR(S) = \frac{1}{18}\left[n(n-1)(2n+5) - \sum_{p=1}^{q} t_p(t_p-1)(2t_p+5)\right], \tag{A5}$$

where q is the number of tied groups and t_p is the number of data values in the p^{th} group. The significance of the trend is obtained from the standard normal cumulative distribution probability tables.

[48] The Sen's method uses a linear model to estimate the slope of the trend, meaning that $f(t)$ in equation (A1) is assumed to be represented by:

$$f(t) = Qt + B, \tag{A6}$$

where Q is the estimated slope and B is a constant. In order to obtain the slope of the trend, first all data value pairs in the time series are calculated according to equation:

$$Q_i = \frac{x_j - x_k}{j - k}, \tag{A7}$$

where $j > k$. The Sen's estimator of slope is the median of all the data pair slopes. The advantages of the Mann-Kendal test and the Sen's method are that missing values are allowed and the data need not conform to any specific distribution. In addition, single data errors or outliers, do not greatly affect the estimated slope by the Sen's method [*Chu et al.*, 2010].

Appendix B: A Classical Nonparametric Test for the Difference in Location

[49] The nonparametric Wilcoxon-Mann-Whitney test is a rank sum test used to evaluate a difference in location between two independent data samples [*Chu and Chen*, 2005]. The statistical significance of the reanalysis II sea level pressure differences between two epochs will be tested using this nonparametric test in which the two batches of data are pooled and ranked. The null hypothesis is that the two batches originate from the same distribution. Assume that there are two batches of sample data, with sample sizes n_1 and n_2. Let U be the Mann-Whitney statistic:

$$\begin{aligned} U_1 &= R_1 - \frac{n_1}{2}(n_1 + 1), \\ U_2 &= R_2 - \frac{n_2}{2}(n_2 + 1) \end{aligned} \tag{B1}$$

where R_1 and R_2 are denoted as the sum of the ranks held by batches 1 and 2 respectively. For a moderately large n_1 and n_2, the null distribution of the Wilcoxon-Mann-Whitney test is approximately Gaussian with:

$$\mu_U = \frac{n_1 n_2}{2} \tag{B2}$$

$$\sigma_U = \left[\frac{n_1 n_2 (n_1 + n_2 + 1)}{12}\right]^{1/2} \tag{B3}$$

[50] Once μ_U, σ_U, and U_1 (or U_2) are estimated, the U statistic at each grid point is transformed into a standard Gaussian variable and is evaluated for its statistical significance [*Chu*, 2002].

[51] **Acknowledgments.** Comments from three anonymous reviewers improved the quality and presentation of this paper. This study is prepared by the Joint Institute for Marine and Atmospheric Research, University of Hawaii, under award NA090AR4320075 from the National Oceanic and Atmospheric Administration (NOAA), U.S. Department of Commerce. The views expressed herein are those of the authors and do not necessarily reflect the views of NOAA or any of its subagencies.

References

Cao, G., T. W. Giambelluca, D. E. Stevens, and T. A. Schroeder (2007), Inversion variability in the Hawaiian trade wind regime, *J. Clim.*, *20*, 1145–1160, doi:10.1175/JCLI4033.1.

Cardone, V. J., J. G. Greenwood, and M. A. Cane (1990), On trends in historical marine wind data, *J. Clim.*, *3*, 113–127, doi:10.1175/1520-0442(1990)003<0113:OTIHMW>2.0.CO;2.

Chen, Y.-L., and A. J. Nash (1994), Diurnal variation of surface airflow and rainfall frequencies on the island of Hawaii, *Mon. Weather Rev.*, *122*, 34–56, doi:10.1175/1520-0493(1994)122<0034:DVOSAA>2.0.CO;2.

Chu, P.-S. (2002), Large-scale circulation features associated with decadal variations of tropical cyclone activity over the central north Pacific, *J. Clim.*, *15*, 2678–2689, doi:10.1175/1520-0442(2002)015<2678:LSCFAW>2.0.CO;2.

Chu, P.-S., and H. Chen (2005), Interannual and interdecadal rainfall variations in the Hawaiian Islands, *J. Clim.*, *18*, 4796–4813, doi:10.1175/JCLI3578.1.

Chu, P.-S., J. Frederick, and A. J. Nash (1991), Exploratory analysis of surface winds in the equatorial western Pacific and El Niño, *J. Clim.*, *4*, 1087–1102, doi:10.1175/1520-0442(1991)004<1087:EAOSWI>2.0.CO;2.

Chu, P.-S., A. J. Nash, and F.-Y. Porter (1993), Diagnostic studies of two contrasting rainfall episodes in Hawaii: Dry 1981 and wet 1982, *J. Clim.*, *6*, 1457–1462, doi:10.1175/1520-0442(1993)006<1457:DSOTCR>2.0.CO;2.

Chu, P.-S., Y.-R. Chen, and T. A. Schroeder (2010), Changes in precipitation extremes in the Hawaiian Islands in a warming climate, *J. Clim.*, *23*, 4881–4900, doi:10.1175/2010JCLI3484.1.

Clarke, A. J., and A. Lebedev (1996), Long-term changes in the equatorial Pacific trade winds, *J. Clim.*, *9*, 1020–1029, doi:10.1175/1520-0442(1996)009<1020:LTCITE>2.0.CO;2.

Collins, M., et al. (2010), The impact of global warming on the tropical Pacific Ocean and El Niño, *Nat. Geosci.*, *3*, 391–397, doi:10.1038/ngeo868.

DiNezio, P. N., A. C. Clement, G. A. Vecchi, B. J. Soden, B. P. Kirtman, and S.-K. Lee (2009), Climate response of the equatorial Pacific to global warming, *J. Clim.*, *22*, 4873–4892, doi:10.1175/2009JCLI2982.1.

Glickman, T. S. (Ed.) (2000), *Glossary of Meteorology*, 2nd ed., *Am. Meteorol. Soc.*, Boston, Mass.

Harrison, D. E. (1989), Post world war II trends in the tropical Pacific surface trades, *J. Clim.*, *2*, 1561–1563, doi:10.1175/1520-0442(1989)002<1561:PWWITI>2.0.CO;2.

Masters, F. J., P. J. Vickery, P. Bacon, and E. N. Rappaport (2010), Toward objective, standardized intensity estimates from surface wind speed observations, *Bull. Am. Meteorol. Soc.*, *91*, 1665–1681, doi:10.1175/2010BAMS2942.1.

Power, S. B., and I. N. Smith (2007), Weakening of the Walker circulation and apparent dominance of El Niño both reach record levels, but has ENSO really changed?, *Geophys. Res. Lett.*, *34*, L18702, doi:10.1029/2007GL030854.

Sanderson, M. (1993), Introduction, in *Prevailing Trade Winds: Weather and Climate in Hawaii*, edited by M. Sanderson, pp. 1–11, Univ. of Hawai'i Press, Honolulu.

Schroeder, T. A. (1981), Characteristics of local winds in northwest Hawaii, *J. Appl. Meteorol.*, *20*, 874–881, doi:10.1175/1520-0450(1981)020<0874:COLWIN>2.0.CO;2.

Schroeder, T. A. (1993), Climate controls, in *Prevailing Trade Winds: Weather and Climate in Hawaii*, edited by M. Sanderson, pp. 12–36, Univ. of Hawai'i Press, Honolulu.

Tokinaga, H., and S.-P. Xie (2011), Wave and anemometer-based sea-surface wind (WASWind) for climate change analysis, *J. Clim.*, *24*, 267–285, doi:10.1175/2010JCLI3789.1.

Vecchi, G. A., and B. J. Soden (2007), Global warming and the weakening of the tropical circulation, *J. Clim.*, *20*, 4316–4340, doi:10.1175/JCLI4258.1.

Wyrtki, K., and G. Meyers (1976), The trade wind field over the Pacific Ocean, *J. Appl. Meteorol.*, *15*, 698–704, doi:10.1175/1520-0450(1976)015<0698:TTWFOT>2.0.CO;2.